Microwave Device Modeling Using Efficient l_1 Optimization: A Novel Approach

JOHN W. BANDLER, FELLOW, IEEE, SHAO HUA CHEN, STUDENT MEMBER, IEEE, AND SHAHROKH DAIJAVAD, STUDENT MEMBER, IEEE

Abstract —A powerful modeling technique which exploits the theoretical properties of the l_1 norm is presented. The concept of multicircuit measurements and its advantages for unique identification of parameters are discussed. Self-consistent models for passive and active devices are achieved by an approach that automatically checks the validity of model parameters obtained from optimization. A set of formulas is presented to evaluate the first-order sensitivities of two-port S-parameters with respect to circuit elements appearing in an admittance or impedance matrix description of linear network equivalents. These formulas are used for devices with linear network models in conjunction with an efficient gradient-based l_1 algorithm. Practical use of the efficient l_1 algorithm in complicated problems for which gradient evaluation may not be feasible is also discussed. Two different optimization problems are formulated which connect the concept of modeling to physical adjustments on the device. Detailed examples in modeling of multicoupled cavity filters and GaAs FET's are presented.

I. Introduction

The PROBLEM of approximating a measured response by a network or system response has been formulated as an optimization problem with respect to the equivalent circuit parameters of a proposed model. The traditional approach in modeling is almost entirely directed at achieving the best possible match between measured and calculated responses. This approach has serious shortcomings in two frequently encountered cases. The first case is when the equivalent circuit parameters are not unique with respect to the responses selected and the second is when nonideal effects are not modeled adequately, the latter causing an imperfect match even if small measurement errors are allowed for. In both cases, a family of solutions for circuit model parameters may exist which produce reasonable and similar matches between measured and calculated responses.

In this paper, we present a new formulation for modeling that automatically checks the validity of the circuit parameters, with a simultaneous attempt in matching measured and calculated responses. If successful, the method provides confidence in the validity of the model parameters; otherwise, it proves their incorrectness. The use of the l_1 norm, based on its theoretical properties, is an integral part of the approach. We discuss the use of an efficient l_1 algorithm [1]–[3] both in problems for which response gradients can be evaluated and in complicated problems for which gradient evaluation is not feasible. The use of a gradient-based l_1 algorithm and of a variation of Broyden's formula to update gradients internally [3] makes it possible to employ a state-of-the-art optimization algorithm with any simulation package capable simply of providing responses. Therefore, widely used microwave design programs, e.g., SUPER-COMPACT [4] and TOUCHSTONE [5], which do not calculate exact gradients, could employ such an algorithm with an appropriate interface. As a result, it is conceivable that the modeling technique described could find its way into microwave engineering practice in the near future.

Two examples of practical interest, namely, modeling of a narrow-band multicoupled cavity filter and of a wide-band GaAs FET, follow the theoretical description of both the traditional and the new approaches. In both examples, a large number of variables are considered.

Manuscript received March 15, 1986; revised June 2, 1986. This work was supported in part by the Natural Sciences and Engineering Research Council of Canada under Grant G1135.

The authors are with the Simulation Optimization Systems Research Laboratory and the Department of Electrical and Computer Engineering, McMaster University, Hamilton, Ont., Canada L8S 4L7. J. W. Bandler is also with Optimization Systems Associates Inc., Dundas, Ont., Canada L9H 6L1.

IEEE Log Number 8610563.

II. Review of Concepts in Approximation

A. The Approximation Problem

The traditional approximation problem is stated as follows

$$\underset{x}{\text{minimize}} \, \| f \| \tag{1}$$

where a typical component of vector f, namely f_i evaluated at the frequency point ω_i, is given by

$$f_i \triangleq w_i \left(F_i^c(x) - F_i^m \right), \qquad i = 1, 2, \cdots, k. \tag{2}$$

F_i^m is a measured response at ω_i and F_i^c is the response of an appropriate network which depends nonlinearly on a vector of model parameters $x \triangleq [x_1 \ \ x_2 \ \ \cdots \ \ x_n]^T$ and w_i denotes a nonnegative weighting factor. Here $\| f \|$ denotes the general l_p norm, given by

$$\| f \| = \left(\sum_{i=1}^{k} |f_i|^p \right)^{1/p}. \tag{3}$$

The widely used least-squares norm, or l_2, is obtained with $p = 2$, and as $p \to \infty$ (1) becomes the well-known minimax problem. In this paper, we are primarily concerned with the l_1 norm, i.e., formulating the approximation problem

0018-9480/86/1200-1282$01.00 ©1986 IEEE

TABLE I
APPROXIMATION PROBLEM USING l_1 AND l_2 OPTIMIZATION

Parameter	Case A ℓ_1	Case A ℓ_2	Case B ℓ_1	Case B ℓ_2	Case C ℓ_1	Case C ℓ_2
x_1	0.0	0.0071	0.0	0.0391	0.0	−0.0261
x_2	8.5629	8.5660	8.6664	5.8050	8.5506	12.8828
x_3	29.3124	29.7515	30.5684	30.0523	29.1070	26.0012
x_4	24.7375	25.0108	25.4261	19.6892	24.6452	32.1023
x_5	12.2285	12.3699	12.9234	21.8794	12.0887	7.4300

as

$$\underset{x}{\text{minimize}} \|f\| \triangleq \sum_{i=1}^{k} |f_i|. \tag{4}$$

B. Properties of l_1 Approximation

The use of the l_1 norm as compared to the other norms l_p with $p>1$ has the distinctive property that some large components of f are ignored; i.e., at the solution there may well be a few f_i's which are much larger than the others. This means that, with the components of f as defined by (2), a few large measurement errors can be tolerated by the l_1 norm better than any other norm. In this paper, we do not need to assume that such large errors exist. We use a formulation in which some components of f are designed to have large values at the solution, thereby justifying the use of l_1. In Section III, we introduce such a formulation using multicircuit measurements where the change in parameters between different circuits forms part of the objective; i.e., they are some of the f_i's. Indeed, these f_i's are expected to have a few large values and many zeros at the solution.

The robustness of the l_1 optimization in dealing with large components of f, as discussed in the literature [2], [6], is the result of a mathematical property related to the necessary conditions for optimality. The solution to (4) is usually situated at a point where one or more of the f_i's equal zero while some large f_i's are in effect ignored completely.

C. Illustration of l_1 Approximation

To illustrate the above property, we consider a rational approximation problem. We obtain a solution to the problem using l_1 and l_2 optimizations. Then, we deliberately create a few large deviations in the actual functions to observe the effect on parameters when large components of f are supposed to be present at the solution. Again, we emphasize that, because of our formulation in Section III, a few large deviations in f_i's are desired and expected. The parameters obtained using the l_1 and l_2 optimizations with and without deviations present are compared.

We want to find the rational approximant of the form [7]

$$K(x)=\frac{x_1+x_2\omega+x_3\omega^2}{1+x_4\omega+x_5\omega^2} \tag{5}$$

to the function $\sqrt{\omega}$ in the interval $\omega \in [0,1]$. Using 51 uniformly spaced sample points on the given interval,

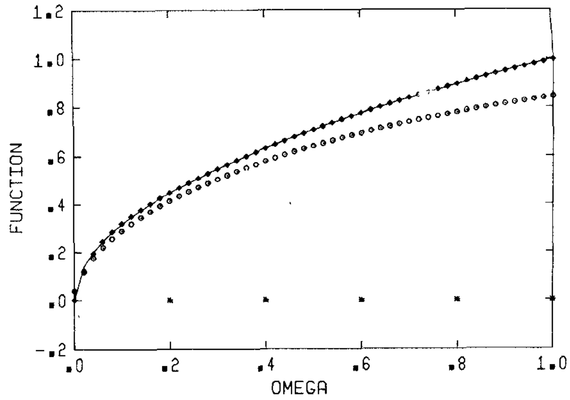

(a)

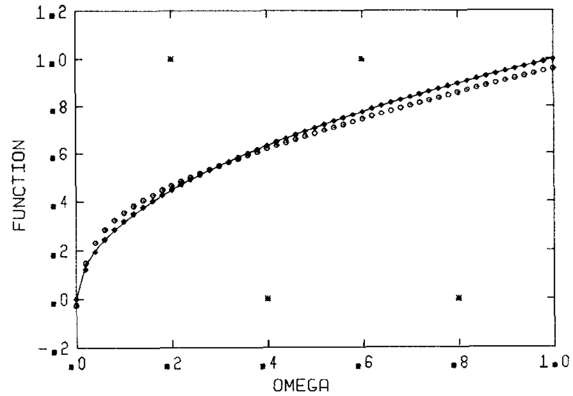

(b)

Fig. 1. Approximations using l_1 and l_2 optimizations. Solid line is the actual function. Diamonds identify the approximation using l_1 and circles represent approximations with l_2. Stars represent data points after large deliberate deviations. (a) and (b) correspond, respectively, to cases B and C in Section II.

parameter vector x was obtained by l_1 and l_2 optimizations and the results are summarized in Table I under case A. Using both sets of parameters, the approximating function virtually duplicates the actual function over the whole interval. We now introduce a few large deviations in the actual function in two separate cases. In case B, the actual function value is replaced by zero at five points in the interval, namely, at 0.2, 0.4, $\cdots$, 1.0. In case C, we use zero at 0.4 and 0.8, and one at 0.2 and 0.6. In both cases, l_1 and l_2 optimizations are performed and the parameters obtained are summarized in Table I.

The parameters obtained by l_1 optimization in cases B and C are consistent with their values in case A. On the other hand, the presence of large deviations has affected the l_2 optimization results severely, and inconsistent parameters are obtained. Fig. 1(a) and (b) illustrates the approximating and actual functions for cases B and C. Whereas the approximation using l_1 has ignored the large deviations completely and has achieved an excellent match for both cases, the l_2 approximation, which was as good as l_1 in case A, has deteriorated. For instance, the particular arrangement of deviations in case B has caused the approximating function to underestimate the actual function over the whole interval.

The property that a few large individual function f_i's are ignored by l_1 optimization and many f_i's are zero at the solution has also found applications in fault-isolation techniques for linear analog circuits [8] and the functional approach to postproduction tuning [9].

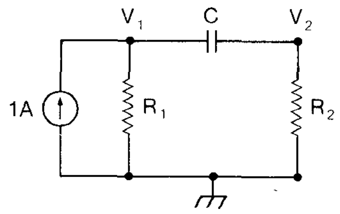

Fig. 2. Simple RC network.

III. New Approach Using Multiple Sets of Measurements

The use of multiple sets of measurements for a circuit was originally thought of by the authors as a way of increasing the "identifiability" of the network. The idea is to overcome the problem of nonuniqueness of parameters that exists when only one set of multifrequency measurements at a certain number of ports (or nodes) is used for identification. By a new set of measurements we mean multifrequency measurements on one or more responses after making a physical adjustment on the device. Such an adjustment results in the deliberate perturbation of one or a few circuit parameters; therefore, to have multiple sets of measurements, multiple circuits differing from each other in one or a few parameters are created. In the above context, the term multicircuit identification may also be used.

In this section, we first use a simple example to illustrate the usefulness of multicircuit measurements in identifying the parameters uniquely. We formulate an appropriate optimization problem and also discuss its limitations. Finally, we develop a model verification method and formulate a second optimization problem which exploits multicircuit measurements and the properties of the l_1 optimization in device modeling.

A. Unique Identification of Parameters Using Multicircuit Measurements

Consider the simple RC passive circuit of Fig. 2. The parameters $x=[R_1 \quad R_2 \quad C]^T$, where T denotes the transpose, are to be identified. If we have measurements only on V_2, given by

$$V_2=\frac{sCR_1R_2}{1+sC(R_1+R_2)} \tag{6}$$

it is clear by inspection that x cannot be uniquely determined regardless of the number of frequency points and the choice of frequencies used. This is because R_1 and R_2 are observed in exactly the same way by V_2. Formally, the nonuniqueness is proved using the concepts discussed in the subject of fault diagnosis of analog circuits [8] in the following way. Given a complex-valued vector of responses $\boldsymbol{h}(x,s_i)$, $i=1,2,\cdots,n_\omega$ (from which real-valued vector $\boldsymbol{F}^c(x,\omega)$ is obtained), the measure of identifiability of x is determined by testing the rank of the $n_\omega \times n$ Jacobian matrix

$$\boldsymbol{J} \triangleq \left[\nabla_x \boldsymbol{h}^T(x)\right]^T. \tag{7}$$

If the rank of matrix $\boldsymbol{J}$ denoted by ρ is less than n, x is not uniquely identifiable from $\boldsymbol{h}$. For the RC circuit example, we have

$$\boldsymbol{J}=\begin{bmatrix} \dfrac{s_1CR_2(1+s_1CR_2)}{[1+s_1C(R_1+R_2)]^2} & \dfrac{s_1CR_1(1+s_1CR_1)}{[1+s_1C(R_1+R_2)]^2} & \dfrac{s_1R_1R_2}{[1+s_1C(R_1+R_2)]^2} \\ \vdots & \vdots & \vdots \\ \dfrac{s_{n_\omega}CR_2(1+s_{n_\omega}CR_2)}{\left[1+s_{n_\omega}C(R_1+R_2)\right]^2} & \dfrac{s_{n_\omega}CR_1(1+s_{n_\omega}CR_1)}{\left[1+s_{n_\omega}C(R_1+R_2)\right]^2} & \dfrac{s_{n_\omega}R_1R_2}{\left[1+s_{n_\omega}C(R_1+R_2)\right]^2} \end{bmatrix}. \tag{8}$$

Denoting the three columns of $\boldsymbol{J}$ by $\boldsymbol{J}_1$, $\boldsymbol{J}_2$, and $\boldsymbol{J}_3$, we have

$$\boldsymbol{J}_1-\left(\frac{R_2}{R_1}\right)^2\boldsymbol{J}_2+\frac{C(R_2-R_1)}{R_1^2}\boldsymbol{J}_3=\boldsymbol{0} \tag{9}$$

i.e., $\boldsymbol{J}$ cannot have a rank greater than 2. Therefore, x is not unique with respect to V_2.

Now, suppose that a second circuit is created when R_2 is adjusted by an unknown amount. Using a superscript to identify the circuit (1 or 2), we have

$$V_2^1=\frac{sC^1R_1^1R_2^1}{1+sC^1\left(R_1^1+R_2^1\right)} \tag{10a}$$

and

$$V_2^2=\frac{sC^1R_1^1R_2^2}{1+sC^1\left(R_1^1+R_2^2\right)} \tag{10b}$$

noting that R_1^2 and C^2 are not present, since only R_2 has changed.

Taking only two frequencies s_1 and s_2, the expanded parameter vector $x=[R_1^1 \quad R_2^1 \quad C^1 \quad R_2^2]^T$ is uniquely identifiable because the Jacobian $\boldsymbol{J}$ given by

$$\boldsymbol{J}=\begin{bmatrix} \frac{s_1C^1R_2^1(1+s_1C^1R_2^1)}{[1+s_1C^1(R_1^1+R_2^1)]^2} & \frac{s_1C^1R_1^1(1+s_1C^1R_1^1)}{[1+s_1C^1(R_1^1+R_2^1)]^2} & \frac{s_1R_1^1R_2^1}{[1+s_1C^1(R_1^1+R_2^1)]^2} & 0 \\ \frac{s_2C^1R_2^1(1+s_2C^1R_2^1)}{[1+s_2C^1(R_1^1+R_2^1)]^2} & \frac{s_2C^1R_1^1(1+s_2C^1R_1^1)}{[1+s_2C^1(R_1^1+R_2^1)]^2} & \frac{s_1R_1^1R_2^1}{[1+s_2C^1(R_1^1+R_2^1)]^2} & 0 \\ \frac{s_1C^1R_2^2(1+s_2C^1R_2^2)}{[1+s_1C^1(R_1^1+R_2^2)]^2} & 0 & \frac{s_1R_1^1R_2^2}{[1+s_1C^1(R_1^1+R_2^2)]^2} & \frac{s_1C^1R_1^1(1+s_1C^1R_1^1)}{[1+s_1C^1(R_1^1+R_2^2)]^2} \\ \frac{s_2C^1R_2^2(1+s_2C^1R_2^2)}{[1+s_2C^1(R_1^1+R_2^2)]^2} & 0 & \frac{s_2R_1^1R_2^2}{[1+s_2C^1(R_1^1+R_2^2)]^2} & \frac{s_2C^1R_1^1(1+s_2C^1R_1^1)}{[1+s_2C^1(R_1^1+R_2^2)]^2} \end{bmatrix} \tag{11}$$

is of rank 4 if $s_1 \neq s_2$.

To summarize the approach, it can be stated that although the use of unknown perturbations adds to the number of unknown parameters, the addition of new measurements could increase the rank of $\boldsymbol{J}$ by an amount greater than the increase in n, thereby increasing the chance of uniquely identifying the parameters. The originality of the technique lies in the fact that neither additional ports (nodes) nor additional frequencies are required. The additional measurements on the perturbed system can be performed at subsets of the ports (nodes) or frequencies employed for the unperturbed system.

Based on the above ideas and for n_c circuits, we formulate an l_1 optimization problem as follows:

$$\underset{\boldsymbol{x}}{\text{minimize}} \sum_{t=1}^{n_c} \sum_{i=1}^{k_t} |f_i^t| \tag{12}$$

where

$$f_i^t \triangleq w_i^t\left[F_i^c(\boldsymbol{x}^t)-(F_i^m)^t\right] \tag{13}$$

and

$$\boldsymbol{x}=\begin{bmatrix} \boldsymbol{x}^1 \\ \boldsymbol{x}_a^2 \\ \vdots \\ \boldsymbol{x}_a^{n_c} \end{bmatrix} \tag{14}$$

with superscript and index t identifying the tth circuit. Here, $\boldsymbol{x}_a^t$ represents the vector of additional parameters introduced after the $(t-1)$th adjustment. It has only one or a few elements compared to n elements in $\boldsymbol{x}^t$ which contains all circuit parameters after the change, i.e., including the ones which have not changed. The variable k_t is an index whose value depends on t; therefore, a different number of frequencies may be used for different circuits.

B. Model Verification Using Multicircuit Measurements

Although the optimization problem formulated in (12) with the variables given in (14) enhances the unique identification of parameters, its limitations should be considered carefully. The limitations are related to the way in which model parameters $\boldsymbol{x}$ are controlled by physical adjustments on the device.

Parameters $\boldsymbol{x}$ are generally controlled by some physical parameters $\boldsymbol{\phi} \triangleq [\phi_1 \quad \phi_2 \quad \cdots \quad \phi_l]^T$. For instance, in active device modeling, intrinsic network parameters are controlled by bias voltages or currents, and in waveguide filters, the penetration of a screw may control a particular element of the network model. The actual functional relationship between $\boldsymbol{\phi}$ and $\boldsymbol{x}$ may not be known; however, we often know which element or elements of $\boldsymbol{x}$ are affected by an adjustment on an element of $\boldsymbol{\phi}$. The success of the optimization problem (12) is dependent on this knowledge; i.e., after each physical adjustment, the correct candidates should be present in $\boldsymbol{x}_a$. To ensure this, we should overestimate the number of model parameters which are likely to change after adjusting an element of $\boldsymbol{\phi}$. On the other hand, we would like to have as few elements as possible in each $\boldsymbol{x}_a$ vector, so that the increase in the number of variables can be overcompensated for by the increase in rank of matrix $\boldsymbol{J}$ resulting from the addition of new measurements.

In practice, by overestimating the number of elements in $\boldsymbol{x}_a$ or by making physical adjustments which indeed affect many model parameters (a change in bias voltage may affect all intrinsic parameters of a transistor model), the optimization problem of (12) may not be better conditioned than the traditional single-circuit optimization. This means that the chance for unique identification of parameters may not increase. However, multicircuit measurements could still be used as an alternative to selecting different frequency points or a greater number of points, as may be done in the single-circuit approach.

We now formulate another optimization problem, which either verifies the model parameters obtained or proves their inconsistency with respect to physical adjustments. The information about which elements of $\boldsymbol{x}$ are affected by adjusting an element of $\boldsymbol{\phi}$, although used to judge the consistency of results, is not required *a priori*. Therefore, the formulation is applicable to all practical cases.

Suppose that we make an easy-to-achieve adjustment on an element of $\boldsymbol{\phi}$ such that one or a few components of $\boldsymbol{x}$ are changed in a dominant fashion and the rest remain constant or change slightly. Consider the following l_1 optimization problem

$$\underset{x}{\text{minimize}} \sum_{t=1}^{2} \sum_{i=1}^{k_t} |f_i^t| + \sum_{j=1}^{n} \beta_j |x_j^1 - x_j^2| \tag{15}$$

where β_j represents an appropriate weighting factor and x is a vector which contains circuit parameters of both the original and perturbed networks, i.e.,

$$x = \begin{bmatrix} x^1 \\ x^2 \end{bmatrix}. \tag{16}$$

Notice that, despite its appearance, (15) can be rewritten easily in the standard l_1 optimization form, which is minimizing $\Sigma|\cdot|$, by taking the individual functions from either the nonlinear part f_i^t or the linear part $x_j^1 - x_j^2$.

The above formulation has the following properties.

1) Considering only the first part of the objective function, the formulation is equivalent to performing two optimizations, i.e., matching the calculated response of the original circuit model with its corresponding measurements and repeating the procedure for the perturbed circuit.

2) By adding the second part to the objective function, we take advantage of the knowledge that only one or a few model parameters should change dominantly by perturbing a component of ϕ. Therefore, we penalize the objective function for any difference between x^1 and x^2. However, since the l_1 norm is used, one or a few large changes from x^1 to x^2 are still allowed. Discussions on the use of the l_1 norm in Section II should be referred to.

The confidence in the validity of the equivalent circuit parameters increases if a) an optimization using the objective function of (15) results in a reasonable match between calculated and measured responses for both circuits 1 and 2 (original and perturbed) and b) the examination of the solution vector x reveals changes from x^1 to x^2 which are consistent with the adjustment to ϕ; i.e., only the expected components have changed significantly. We can build upon our confidence even more by generalizing the technique to more adjustments to ϕ, i.e., formulating the optimization problem as

$$\underset{x}{\text{minimize}} \sum_{t=1}^{n_c} \sum_{i=1}^{k_t} |f_i^t| + \sum_{t=2}^{n_c} \sum_{j=1}^{n} \beta_j^t |x_j^1 - x_j^t| \tag{17}$$

when n_c circuits and their corresponding sets of responses, measurements, and parameters are considered and the first circuit is the reference model before any adjustment to ϕ. In this case, x is given by

$$x = \begin{bmatrix} x^1 \\ x^2 \\ \vdots \\ x^{n_c} \end{bmatrix}. \tag{18}$$

By observing inconsistencies in changes of x with the actual change in ϕ, the new technique exposes the existence of nonideal effects not taken into account in the model. Having confidence in the parameters as well as observing a good match between measured and modeled responses means that the parameters and the model are valid, even if different responses or different frequency ranges are used.

IV. Practical Application of the l_1 Algorithm

Consider the l_1 optimization problem formulated in (17). The success of the new technique described relies upon the use of an efficient and robust l_1 algorithm. Recently, a superlinearly convergent algorithm for nonlinear l_1 optimization has been described [1]. The algorithm, based on the original work of Hald and Madsen [2], is a combination of a first-order method that approximates the solution by successive linear programming and a quasi-Newton method using approximate second-order information to solve the system of nonlinear equations resulting from the first-order necessary conditions for an optimum.

The most efficient use of the l_1 algorithm requires the user to supply function and gradient values of the individual functions in (17); i.e., network responses as well as their gradients are needed. Starting with the impedance or nodal admittance description of a network for which only input and output port responses are of interest, we have derived analytical formulas for evaluation of first-order sensitivities of two-port S parameters with respect to any circuit parameter appearing in the impedance or admittance matrix. The formulas and more explanation are given in the Appendix.

In many practical problems, e.g., in the presence of nonlinear devices or complicated field problems, the evaluation of gradients is not feasible. In such cases, it is possible to estimate the gradients using the numerical difference method. However, this is computationally slow and consequently expensive. To take advantage of a fast gradient-based approach, without requiring user-supplied gradients or using the numerical difference method, the original l_1 algorithm has been modified [3]. Different and flexible versions of the modified algorithm exist. A typical version estimates the gradients using the numerical difference method only once and updates the gradients with minimum extra effort by applying a variation of Broyden's formula as the optimization proceeds. All approximations are performed internally; therefore, the optimization could be linked to any analysis program which provides only the responses.

V. Examples

A. Modeling of Multicoupled Cavity Filters

Test 1: A sixth-order multicoupled cavity filter centered at 11785.5 MHz with a 56.2-MHz bandwidth is considered. Measurements on input and output return loss, insertion loss, and group delay of an optimally tuned filter and the same filter after a deliberate adjustment on the screw which dominantly controls coupling M_{12} were provided by ComDev Ltd., Cambridge, Canada [10]. Although the passband return loss changes significantly, we anticipate

TABLE II
RESULTS FOR THE SIXTH-ORDER FILTER EXAMPLE

Coupling	Original Filter	Perturbed Filter	Change in Parameter
M_{11}	-0 0473	-0 1472	-0 0999*
M_{22}	-0 0204	-0 0696	-0 0492*
M_{33}	-0 0305	-0 0230	0 0075
M_{44}	0 0005	0 0066	0 0061
M_{55}	-0 0026	0 0014	0 0040
M_{66}	0 0177	-0 0047	-0 0224
M_{12}	0.8489	0 7119	-0 1370*
M_{23}	0 6064	0 5969	-0 0095
M_{34}	0 5106	0 5101	-0 0005
M_{45}	0 7709	0 7709	0 0000
M_{56}	0 7898	0 7806	-0 0092
M_{36}	-0 2783	-0 2850	-0 0067

*Significant change in parameter value.

that such a physical adjustment affects only model parameters M_{12}, M_{11}, and M_{22} (the last two correspond to cavity resonant frequencies) in a dominant fashion, possibly with slight changes in other parameters.

Using the new technique described in this paper, we simultaneously processed measurements on passband return loss (input reflection coefficient with a weighting of 1) and stopband insertion loss (with a weighting of 0.05) of both filters, i.e., the original and perturbed models. The l_1 algorithm with exact gradients was used. The evaluation of sensitivities is discussed in detail by Bandler *et al.* [11]. The model parameters identified for the two filters are summarized in Table II. Figs. 3 and 4 illustrate the measured and modeled responses of the original filter and the filter after adjustment, respectively. An examination of the results in Table II and Figs. 3 and 4 shows that not only an excellent match between measured and modeled responses has been achieved, but also the changes in parameters are completely consistent with the actual physical adjustment. Therefore, by means of only one optimization, we have built confidence in the validity of the equivalent circuit parameters. The problem involved 84 nonlinear functions (42×2 responses for original and perturbed filters), 12 linear functions (change in parameters of two circuit equivalents), and 24 variables. The solution was achieved in 72 s of CPU time on the VAX 11/780 system.

Test 2: In this test, we used the new modeling technique to reject a certain set of parameters obtained for an eighth-order multicavity filter by proving their inconsistent behavior with respect to physical adjustments. We then improved the model by including an ideally zero stray coupling in the model and obtained parameters which not only produce a good match between measured and modeled responses, but also behave consistently when perturbed by a physical adjustment.

The eight-order filter is centered at 11 902.5 MHz with a 60-MHz bandwidth. Return loss and insertion loss

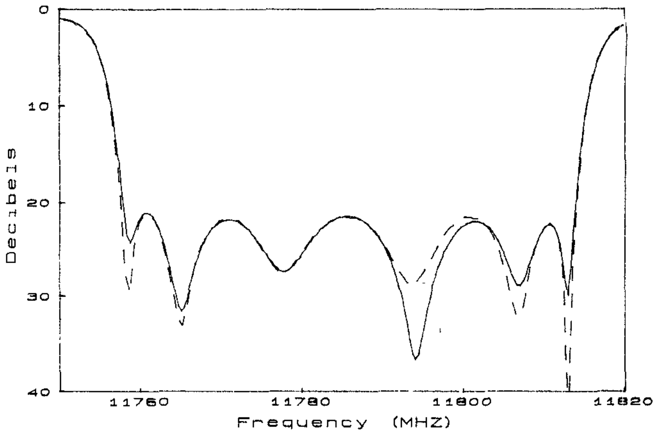

(a)

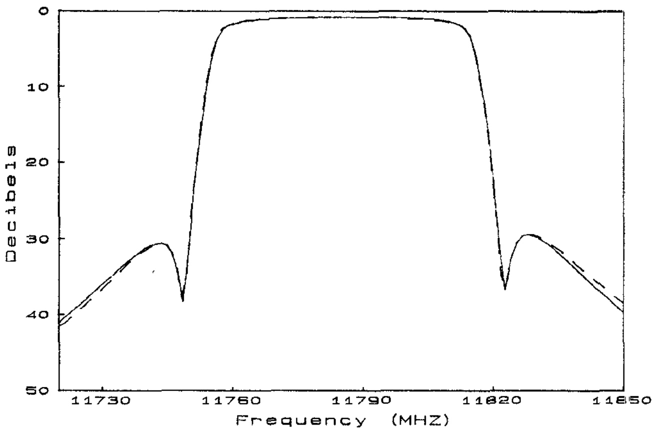

(b)

Fig. 3. (a) Input return loss and (b) insertion loss responses of the sixth-order filter before adjusting the screw. Solid line represents the modeled response and dashed line shows measurement data.

measurements of an optimally tuned filter and the same filter after an adjustment on the iris which dominantly controls coupling M_{23} were provided by ComDev Ltd [10]. Based on the physical structure of the filter, screw couplings M_{12}, M_{34}, M_{56}, and M_{78} and the iris couplings M_{23}, M_{14}, M_{45}, M_{67}, and M_{58}, as well as all cavity resonant frequencies and input–output couplings (transformer ratios), are anticipated as possible nonzero parameters to be identified.

In the first attempt, the stray coupling M_{36} was ignored and passband measurements on input and output return loss and stopband isolation for both filters were used to identify the parameters of the filters. The parameters are summarized in Table III. An examination of the results shows no apparent trend for the change in parameters; i.e., it would have been impossible to guess the source of perturbation (adjustment on the iris controlling M_{23}) from these results. This is the kind of inconsistency that would not have been discovered if only the original circuit had been considered.

In a second attempt, we included the stray coupling M_{36} in the circuit model and processed exactly the same measurements as before. Table III also contains the identified parameters of the two filters for this case. A compari-

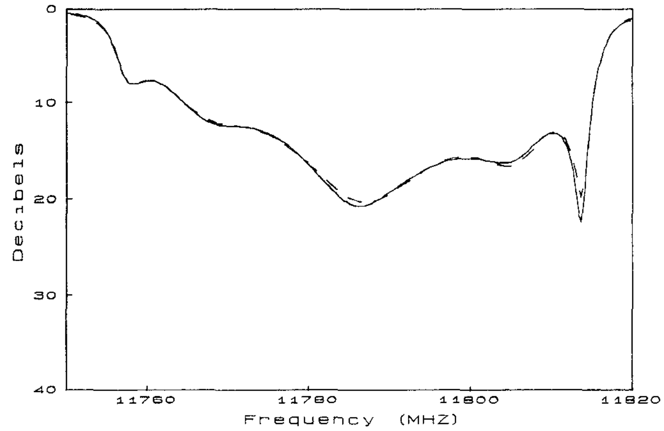

(a)

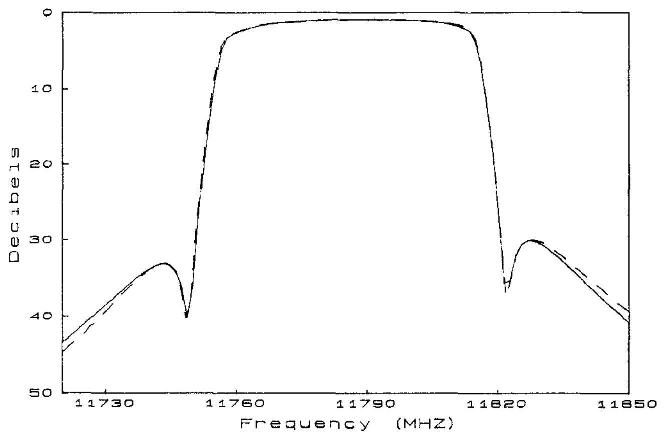

(b)

Fig. 4. (a) Input return loss and (b) insertion loss responses of the sixth-order filter after adjusting the screw. Solid line represents the modeled response and dashed line shows measurement data.

TABLE III
RESULTS FOR THE EIGHTH-ORDER FILTER EXAMPLE

	M_{36} ignored		M_{36} present	
Coupling	Original	Perturbed	Original	Perturbed
M_{11}	−0 0306	−0 1122	−0 0260	−0 0529
M_{22}	0 0026	−0 0243	0 0354	0 6503*
M_{33}	−0 0176	−0 0339	−0 0674	−0 6113*
M_{44}	−0 0105	−0 0579	−0 0078	−0 0151
M_{55}	−0 0273	−0 0009	−0 0214	0 0506
M_{66}	−0 0256	0 0457	−0 0179	−0 0027
M_{77}	−0 0502	0 0679	−0 0424	−0 0278
M_{88}	−0 0423	0 0594	−0 0426	−0 0272
M_{12}	0 7789	0 7462	0 3879	0 2876*
M_{23}	0 8061	0 8376	0 9990	0 8160*
M_{34}	0 4460	0 4205	0 0270	−0 1250*
M_{45}	0 5335	0 5343	0 4791	0 5105
M_{56}	0 5131	0 5373	0 5006	0 5026
M_{67}	0 7260	0 7469	0 6495	0 6451
M_{78}	0 8330	0 8476	0 8447	0 8463
M_{14}	0 3470	−0 3582	−0 7648	−0 7959
M_{58}	−0 1995	−0 1892	−0 1000	−0 0953
M_{36}	-	-	0 1314	0 1459

Input and output couplings: $n_1^2 = n_2^2 = 1.067$.
*Significant change in parameter value.

son of the original and perturbed filter parameters reveals that the significant change in couplings M_{12}, M_{23}, and M_{34} and cavity resonant frequencies M_{22} and M_{33} is absolutely consistent with the actual adjustment on the iris; i.e., by inspecting the change in parameters, it is possible to deduce which iris has been adjusted. The measured and modeled input return loss and insertion loss responses of the two filters are illustrated in Figs. 5 and 6. It is interesting to mention that the match between measured and modeled responses in the first attempt, where M_{36} was ignored and inconsistent parameters were found, is almost as good as the match in Figs. 5 and 6. This justifies the essence of this paper, which attempts to identify the most consistent set of parameters among many that produce a reasonable match between measured and calculated responses.

B. FET Modeling

Test 1: Device NEC700, for which measurement data are supplied with TOUCHSTONE, was considered. Using S-parameter data, single-circuit modeling with the l_1 objective was performed. The goal of this experiment was to prepare for the more complicated Test 2 by testing some common formulas and assumptions. The equivalent circuit at normal operating bias (including the carrier) with 16 possible variables, as illustrated in Fig. 7, was used. An l_1 optimization with exact gradients, which are evaluated using the formulas derived in the Appendix, was performed. Measurement data were taken from 4 to 20 GHz. Table IV summarizes the identified parameters and Fig. 8 illustrates the measured and modeled responses.

Test 2: Using S-parameter data for the device B1824-20C from 4 to 18 GHz, Curtice and Camisa have achieved a very good model for the FET chip [12]. They have used the traditional least squares optimization of responses utilizing SUPER-COMPACT. Their success is due to the fact that they have reduced the number of possible variables in Fig. 7 from 16 to 8 by using dc and zero-bias measurements. We created two sets of artificial S-parameter measurements with TOUCHSTONE: one set using the parameters reported by Curtice and Camisa (operating bias $V_{ds} = 8.0$ V, $V_{gs} = -2.0$ V, and $I_{ds} = 128.0$ mA) and the other by changing the values of C_1, C_2, L_g, and L_d to simulate the effect of taking different reference planes for the carriers. Both sets of data are shown in Fig. 9, where the S parameters of the two circuits are plotted on a Smith Chart.

Using the technique described in this paper, we processed the measurements on the two circuits simultaneously by minimizing the function defined in (15). The objective of this experiment is to show that even if the equivalent circuit parameters were not known, as is the case using real measurements, the consistency of the results would be

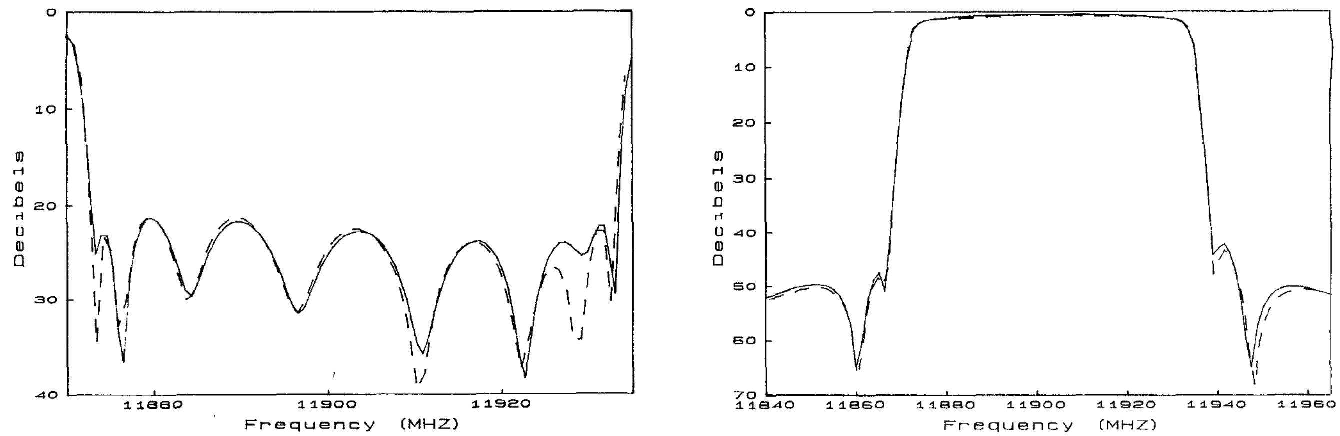

(a) (b)

Fig. 5. (a) Input return loss and (b) insertion loss of the eighth-order filter before adjusting the iris. Solid line represents the modeled response and dashed line shows the measurement data.

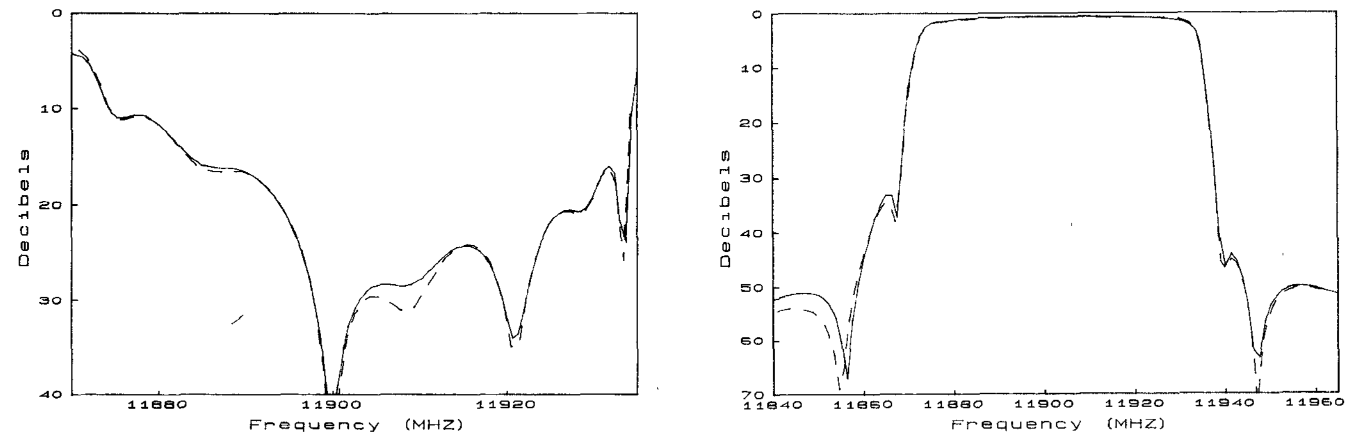

(a) (b)

Fig. 6. (a) Input return loss and (b) insertion loss of the eighth-order filter after adjusting the iris. Solid line represents the modeled response and dashed line shows the measurement data.

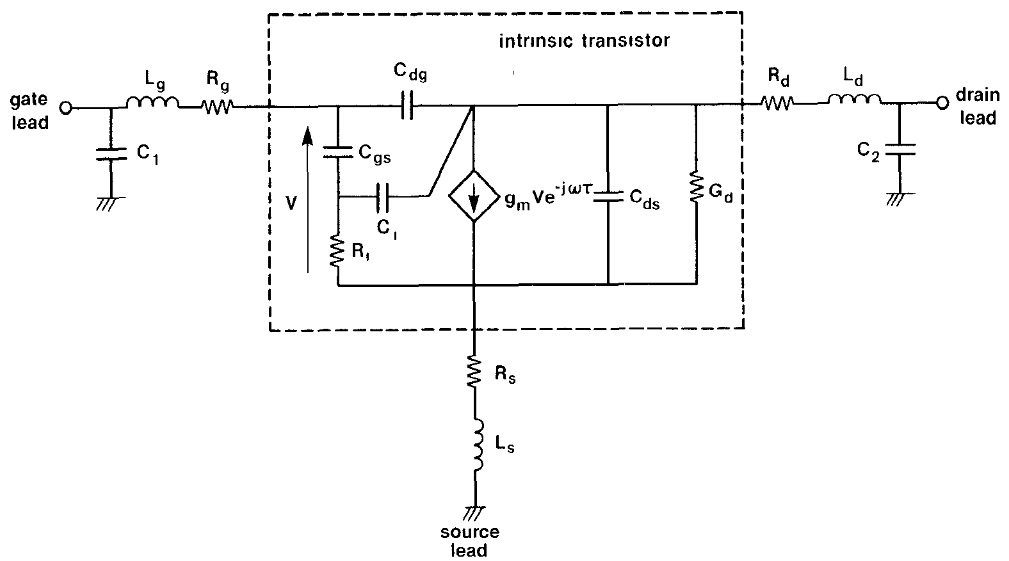

Fig. 7. Equivalent circuit of carrier-mounted FET.

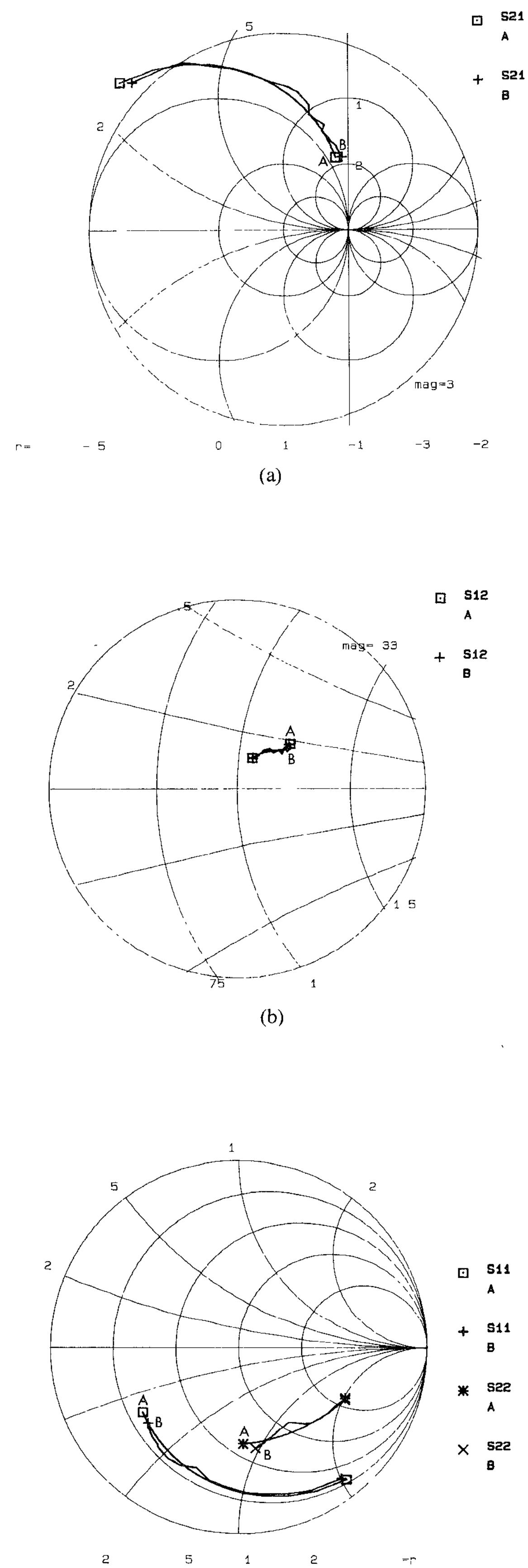

Fig. 8. Smith Chart display of S_{11}, S_{22}, S_{12}, and S_{21} in modeling of NEC700. The frequency range is 4–20 GHz. Points A and B mark the high-frequency end of modeled and measured responses, respectively.

TABLE IV
RESULTS FOR THE NEC700 FET EXAMPLE

Parameter	Value
C_1 (pF)	0 0448
C_2 (pF)	0 0058
C_{dg} (pF)	0 0289
C_{gs} (pF)	0 2867
C_{ds} (pF)	0 0822
C_i (pF)	0 0100
R_g (Ω)	3 5000
R_d (Ω)	2 0000
R_s (Ω)	3 6270
R_i (Ω)	7 3178
G_d^{-1} (kΩ)	0 2064
L_g (nH)	0 0585
L_d (nH)	0 0496
L_s (nH)	0 0379
g_m (S)	0 0572
τ (ps)	3 1711

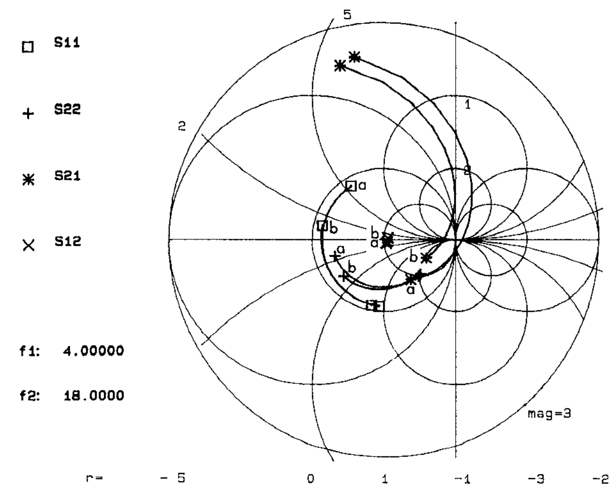

Fig. 9. Smith Chart display of S_{11}, S_{22}, S_{12}, and S_{21} for the carrier-mounted FET device B1824-20C before and after adjustment of parameters. Points a and b mark the high-frequency end of original and perturbed network responses, respectively.

proved only if the intrinsic parameters of the FET remain unchanged between the two circuits. This was indeed the case for the experiment performed. Although the maximum number of possible variables, namely 32 (16 for each circuit), was allowed for in the optimization, the intrinsic parameters were found to be the same between the two circuits and, as expected, C_1, C_2, L_g, and L_d changed from circuit 1 to 2. Table V summarizes the parameter values obtained. The problem involved 128 nonlinear functions (real and imaginary parts of four S parameters, at eight frequencies, for two circuits), 16 linear functions, and 32 variables. The CPU time on the VAX 11/780 system was 79 s.

TABLE V
RESULTS FOR THE GaAs FET B1824-20C EXAMPLE

Parameter		Original Circuit	Perturbed Circuit
C_1	(pF)	0 0440	0 0200*
C_2	(pF)	0 0389	0 0200*
C_{dg}	(pF)	0 0416	0 0416
C_{gs}	(pF)	0 6869	0 6869
C_{ds}	(pF)	0 1900	0 1900
C_i	(pF)	0 0100	0 0100
R_g	(Ω)	0 5490	0 5490
R_d	(Ω)	1 3670	1 3670
R_s	(Ω)	1 0480	1 0480
R_i	(Ω)	1 0842	1 0842
G_d^{-1}	(kΩ)	0 3761	0 3763
L_g	(nH)	0 3158	0 1500*
L_d	(nH)	0 2515	0 1499*
L_s	(nH)	0 0105	0 0105
g_m	(S)	0 0423	0 0423
τ	(ps)	7.4035	7 4035

*Significant change in parameter value.

VI. CONCLUSIONS

We have described a new technique for the modeling of microwave devices which exploits multicircuit measurements. The way in which the multicircuit measurements may contribute to the unique identification of parameters has been described mathematically with the help of a simple example. An optimization problem which is directly aimed at overcoming the nonuniqueness of parameters was formulated. A second formulation, which is aimed at the automatic verification of model parameters by checking the consistency of their behavior with respect to physical adjustments on the device, was proposed.

The use of the l_1 norm is an integral part of the approach. We discussed the use of an efficient l_1 algorithm both in problems for which gradient evaluation is possible (a set of useful formulas was presented) and in complicated problems for which gradient evaluation is not feasible. In the latter case, the technique described in this paper can be used in conjunction with widely used microwave design programs or in-house analysis programs employed in industry.

An important aspect of any optimization problem is the question of starting values. To address this problem, we recommend the use of l_1 optimization with simplified network equivalent models such as low-frequency models. In cases where little information about the range of parameter values is available, a common set of measurements can be used with different network equivalents (different topology) for the optimization. The solutions obtained using simplified models provide good starting values for multicircuit modeling with complicated network equivalents.

The results for the modeling of narrow-band multicoupled cavity filter and wide-band GaAs FET examples are very promising and completely justify the use of our multicircuit approach and formulation. The authors strongly believe that the use of multiple sets of measurements and a formulation which ties modeling (performed by computer) to the actual physical adjustments on the device will enhance further developments in modeling and tuning of microwave circuits.

ACKNOWLEDGMENT

The authors are pleased to acknowledge the assistance of R. Tong and H. AuYeung of ComDev Ltd., Cambridge, Canada, in preparing measurement data for multicoupled cavity filters.

APPENDIX
FIRST-ORDER SENSITIVITY EVALUATION FOR TWO-PORT S PARAMETERS

Here, the details for evaluating the first-order sensitivities of two-port S parameters with respect to the circuit elements are given. It is assumed that the nodal admittance matrix $\boldsymbol{Y}$ for the circuit model is available. For the case in which the impedance matrix is given, the approach is similar.

The open-circuit impedance matrix of the two-port is given by

$$z_{OC}=\begin{bmatrix}(\boldsymbol{Y}^{-1})_{11} & (\boldsymbol{Y}^{-1})_{1n}\\ (\boldsymbol{Y}^{-1})_{n1} & (\boldsymbol{Y}^{-1})_{nn}\end{bmatrix} \tag{A1}$$

where $\boldsymbol{Y}_{n\times n}$ is the admittance matrix arranged such that nodes 1 and n identify the ports at which S parameters are of interest.

Assuming that ϕ is a generic notation for a variable which appears in $\boldsymbol{Y}$ in the locations as shown below

$$\boldsymbol{Y}=\begin{array}{c}\\ \\ i\\ \\ j\\ \\ \end{array}\begin{array}{c}\begin{array}{ccccc} & k & & l & \end{array}\\ \left[\begin{array}{ccccc} & \vdots & & \vdots & \\ \cdots & \phi & \cdots & -\phi & \cdots\\ & \vdots & & \vdots & \\ \cdots & -\phi & \cdots & \phi & \cdots\\ & \vdots & & \vdots & \end{array}\right]\end{array} \tag{A2}$$

it can be proved, after a few simple algebraic manipulations, that

$$z_{OC}=\begin{bmatrix}p_1 & q_1\\ p_n & q_n\end{bmatrix} \tag{A3}$$

and

$$\frac{\partial z_{OC}}{\partial\phi}=-\begin{bmatrix}(\hat{p}_i-\hat{p}_j)(p_k-p_l) & (\hat{p}_i-\hat{p}_j)(q_k-q_l)\\ (\hat{q}_i-\hat{q}_j)(p_k-p_l) & (\hat{q}_i-\hat{q}_j)(q_k-q_l)\end{bmatrix} \tag{A4}$$

where vectors $\boldsymbol{p}$, $\hat{\boldsymbol{p}}$, $\boldsymbol{q}$, and $\hat{\boldsymbol{q}}$ are obtained by solving the systems of equations

$$\boldsymbol{Y}\boldsymbol{p} = \boldsymbol{e}_1 \tag{A5a}$$

$$\boldsymbol{Y}^T\hat{\boldsymbol{p}} = \boldsymbol{e}_1 \tag{A5b}$$

$$\boldsymbol{Y}\boldsymbol{q} = \boldsymbol{e}_n \tag{A5c}$$

and

$$\boldsymbol{Y}^T\hat{\boldsymbol{q}} = \boldsymbol{e}_n \tag{A5d}$$

where $\boldsymbol{e}_1 = [\,1\;0\cdots 0]^T$ and $\boldsymbol{e}_n = [0\cdots 0\;1]^T$.

From a computational point of view, the solution to (A.5) requires only one LU factorization of $\boldsymbol{Y}$ (the LU factors of $\boldsymbol{Y}^T$ are obtained from LU factors of $\boldsymbol{Y}$ without calculations) and four forward and backward substitutions. Matrix $\boldsymbol{Y}$ is never inverted in the process.

The two-port S-parameter matrix and its sensitivities with respect to ϕ are then evaluated using the following relationships:

$$(\bar{z} - \boldsymbol{1}) = \boldsymbol{S}(\bar{z} + \boldsymbol{1}) \tag{A6}$$

and

$$\frac{\partial \boldsymbol{S}}{\partial \phi} = \frac{1}{2Z_0}(\boldsymbol{1} - \boldsymbol{S})\frac{\partial z_{OC}}{\partial \phi}(\boldsymbol{1} - \boldsymbol{S}) \tag{A7}$$

where

$$\bar{z} = \frac{1}{Z_0} z_{OC} \tag{A8}$$

and

$$\boldsymbol{S} = \begin{bmatrix} S_{11} & S_{12} \\ S_{21} & S_{22} \end{bmatrix} \tag{A9}$$

with Z_0 denoting the normalizing impedance and $\boldsymbol{1}$ representing the 2×2 unit matrix.

The sensitivities of $\boldsymbol{S}$ with respect to circuit elements can be evaluated using $\partial \boldsymbol{S}/\partial \phi$. For instance, for transconductance parameter g_m and delay τ associated with a VCCS in the circuit, we have $\partial \boldsymbol{S}/\partial g_m = e^{-j\omega\tau}\,\partial \boldsymbol{S}/\partial \phi$ and $\partial \boldsymbol{S}/\partial \tau = -\,j\omega g_m e^{-j\omega\tau}\,\partial \boldsymbol{S}/\partial \phi$, where $\phi = g_m e^{-j\omega\tau}$.

References

[1] J. W. Bandler, W. Kellermann, and K. Madsen, "A superlinearly convergent algorithm for nonlinear l_1 optimization with circuit applications," in *Proc. IEEE Int. Symp. Circuits and Systems* (Kyoto, Japan), 1985, pp. 977–980.

[2] J. Hald and K. Madsen, "Combined LP and quasi-Newton methods for nonlinear l_1 optimization," *SIAM J. Numer. Anal.*, vol. 22, pp. 68–80, 1985.

[3] J. W. Bandler, S. H. Chen, S. Daijavad, and K. Madsen, "Efficient gradient approximations for nonlinear optimization of circuits and systems," in *Proc. IEEE Int. Symp. Circuits and Systems* (San Jose, CA), 1986, pp. 964–967.

[4] *SUPER-COMPACT User's Manual*, COMSAT General Integrated Systems Inc., Palo Alto, CA, 1984.

[5] TOUCHSTONE User's Manual, EEsof Inc., Westlake Village, CA, 1986.

[6] R. H. Bartels and A. R. Conn, "An approach to nonlinear l_1 data fitting," Computer Science Department, University of Waterloo, Rep. CS-81-17, 1981.

[7] R. A. El-Attar, M. Vidyasagar, and S. R. K. Dutta, "An algorithm for l_1-norm minimization with application to nonlinear l_1-approximation," *SIAM J. Numer. Anal.*, vol. 16, pp. 70–86, 1979.

[8] J. W. Bandler and A. E. Salama, "Fault diagnosis of analog circuits," *Proc. IEEE*, vol. 73, pp. 1279–1325, 1985.

[9] J. W. Bandler and A. E. Salama, "Functional approach to microwave postproduction tuning," *IEEE Trans. Microwave Theory Tech.*, vol. MTT-33, pp. 302–310, 1985.

[10] ComDev Ltd., 155 Sheldon Drive, Cambridge, Ontario, Canada N1R 7H6, private communication, 1985.

[11] J. W. Bandler, S. H. Chen, and S. Daijavad, "Exact sensitivity analysis for optimization of multi-coupled cavity filters," *Int. J. Circuit Theory and Applic.*, vol. 14, pp. 63–77, 1986.

[12] W. R. Curtice and R. L. Camisa, "Self-consistent GaAs FET models for amplifier design and device diagnostics," *IEEE Trans. Microwave Theory Tech.*, vol. MTT-32, pp. 1573–1578, 1984.

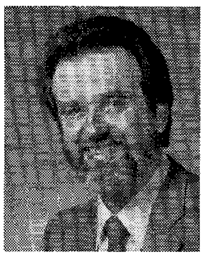

John W. Bandler (S'66–M'66–SM'74–F'78) was born in Jerusalem, Palestine, on November 9, 1941. He studied at Imperial College of Science and Technology, London, England, from 1960–1966. He received the B.Sc. (Eng.), Ph.D., and D.Sc. (Eng.) degrees from the University of London, London, England, in 1963, 1967, and 1976, respectively.

He joined Mullard Research Laboratories, Redhill, Surrey, England, in 1966. From 1967 to 1969, he was a postdoctorate fellow and sessional lecturer at the University of Manitoba, Winnipeg, Canada. He joined McMaster University, Hamilton, Canada, in 1969, where he is currently a Professor of electrical and computer engineering. He has served as Chairman of the Department of Electrical Engineering and Dean of the Faculty of Engineering. He currently directs research, which has received substantial support by the Natural Sciences and Engineering Research Council of Canada under its Operating and Strategic Grants Awards, in the Simulation Optimization Systems Research Laboratory. Dr. Bandler is also currently president of Optimization Systems Associates, Inc. He has provided consulting services and software to numerous organizations in the electronic, microwave, and electrical power industry, specializing in advanced applications of simulation, sensitivity analysis, and mathematical optimization techniques.

Dr. Bandler is a contributor to *Modern Filter Theory and Design* (Wiley-Interscience, 1973). He has more than 210 publications, four of which appear in *Computer-Aided Filter Design* (IEEE Press, 1973), one in *Microwave Integrated Circuits* (Artech House, 1985), and one in *Low-Noise Microwave Transistors and Amplifiers* (IEEE Press, 1981). Dr. Bandler was an Associate Editor of the IEEE TRANSACTIONS ON MICROWAVE THEORY AND TECHNIQUES (1969–1974). He was Guest Editor of the special issue of the IEEE TRANSACTIONS ON MICROWAVE THEORY AND TECHNIQUES on Computer-Oriented Microwave Practices (March 1974). Dr. Bandler is a Fellow of the Royal Society of Canada and of the Institution of Electrical Engineers (Great Britain). He is a member of the Association of Professional Engineers of the Province of Ontario (Canada).

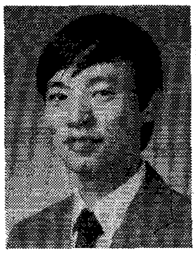

Shao Hua Chen (S'84) was born in Swatow, Guangdong, China, on September 27, 1957. He received the B.S. degree from South China Institute of Technology, Guangzhou, China, in 1982.

From July 1982 to August 1983, he was with the Department of Automation, South China Institute of Technology, Guangzhou, China, as a teaching assistant. He was awarded a Chinese Government Scholarship and joined the Department of Electrical and Computer Engineering, McMaster University, Hamilton, Canada, in September 1983, where he is currently a teaching assistant and graduate student working towards the Ph.D. degree. He has been awarded an Ontario Graduate Scholarship for the academic years 1985/86 and 1986/87. His research interests are in optimization methods, sensitivity analysis, modeling, tuning, and CAD software on personal computers.

Shahrokh Daijavad (S'82) was born in Isfahan, Iran, on July 7, 1960. He received the B.Eng. (summa cum laude) and Ph.D. degrees in electrical engineering from McMaster University, Hamilton, Ontario, Canada, in 1983 and 1986, respectively.

From 1983 to 1986, he worked as a teaching assistant in the Department of Electrical and Computer Engineering, McMaster University, while holding an Ontario Graduate Scholarship from 1983 to 1985 and a Natural Sciences and Engineering Research Council of Canada Scholarship from 1985 to 1986. His research interests are in computer-aided design with emphasis on applications of optimization theory in modeling, fault location, and tuning.